High contrast imaging for weakly diffracting specimens with ptychographical iterative engine

Xingchen Pan,[1] Suhas P. Veetil,[2] Cheng Liu,[1,*] and Jianqiang Zhu[1]

[1]*Shanghai Institute of Optics and Fine Mechanics, ChineseAcademy of Sciences, Shanghai 201800, China*

[2]*Department of Physics, AmityUniversityDubai, Dubai 345019, United Arab Emirates*

**Corresponding author: chengliu@siom.ac.cn*

Received May 9, 2012; revised June 26, 2012; accepted June 26, 2012;
posted July 2, 2012 (Doc. ID 168306); published August 6, 2012

As a newly developed coherent diffraction-imaging (CDI) imaging method, the ptychographical iterative engine not only can bypass the difficulty of having high-quality optics in x-ray microscopy by a numerical reconstruction algorithm, but also has obvious advantages on traditional CDI methods in both converging speeds and view fields. However, like in the other CDI methods, the reconstruction of the image from the intensity data of a weakly diffracting specimen is still difficult because of the low signal to noise ratio. To improve this situation, a modification to the currently used algorithms is suggested to double the presence of high spatial frequencies in the diffraction pattern and accordingly to enhance the contrast and fine details of the reconstructions. The simulation and experimental results are presented, and the results can be extended to other CDI methods also.

OCIS codes: 100.3190, 100.5070, 110.3010, 180.0180.

Recent advances in transmission microscopy have led to the evolution of a "lensless" technique for 2-, and 3-dimensional reconstruction of the image of nanoscale structures such as proteins, nanotubes, nanocrystals, and defects. The technique is widely referred to as coherent diffractive imaging (CDI) [1–5]. In this method, the objective lens is removed and a detector is placed in the far-field. Then it is still possible to calculate the object structure via certain iterative phase retrieval algorithms despite the loss of phase information in the recorded data [2–6]. This is the basic principle of CDI algorithm. Theoretically, CDI allows one to obtain the resolution ultimately limited only by the wavelength of radiation used and not by the optics quality. Due to this outstanding advantage, CDI has become an important research topic in the field of imaging with x-rays and electrons [6–8].

The traditional CDI method suffers from the disadvantages in view field, converging speed, and reliability. To overcome these disadvantages, Rodenburg proposed the PIE ptychographical iterative engine (PIE) algorithm, which uses a Wegener filter like algorithm to reconstruct the image iteratively from a set of diffraction patterns [9–12]. By combing the advantages of CDI and traditional phychography algorithms, PIE has much faster converging speed and wider view field than the common CDI method. By now PIE has achieved great progress in imaging with light, x-rays, and electrons. Like the common CDI method, one important advantage of PIE lies on its ability to measure the phase distribution directly from the far-field diffraction patterns. However, for weakly diffraction samples, the contrast of the reconstructed phase image is very low, and it is difficult to observe fine details in the specimen's structure due to the noise presence. Thus, exploring new methods to enhance the image contrast becomes very meaningful. In this paper we suggest the use of divergent light beams for the illumination in the data recording process and a modified PIE algorithm for the image reconstruction to get a remarkable contrast enhancement. The results obtained can also be extended to other CDI techniques.

The optical setup for the PIE technique is schematically shown in Fig. 1. The specimen with a transmission function $q(r)$ is fixed on a translation stage and is illuminated by a complex-valued illuminating probe wave front. We can also define the wave exiting the specimen as $\psi_e(r,R) = q(r)P(r-R)$ which is indeed an overlap of specimen transmission function and probe function. For both x-ray and electron microscopy, the wavelength is quite small, for example the wavelength of a 200 kV electron is 0.025 Å. In most of the real experiments, the distance between the CCD array and the sample is about 10 cm, and the CCD always records the Fraunhofer diffraction of the sample. The recorded intensity, $I(k)$ is the square of the Fourier transform of the $\psi_e(r,R)$, that is, $I(k) = |\mathrm{FFT}[\psi_e(r,R)]|^2$, where k is the reciprocal space coordinates of the real-space coordinate r, and the fast Fourier transform. This is the reason why the CCD is placed on the back focal plane of a lens in Fig. 1 to record the diffraction patterns.

The far-field intensities are recorded for different sample-to-probe positions shifted by a vector R. The phase retrieval is started with a random guess for the transmission function $q(r)$. The detailed iteration reconstruction procedure can be found in [9]. Since the diffraction pattern is obtained by the interference between the zero-order beam $A_0(k)$ and the diffracted beam $A_d(k)$, we can rewrite intensity of the diffraction pattern as

$$\begin{aligned} I(k) &= |A_0(k)+A_d(k)|^2 \\ &= |A_0(k)|^2 + 2|A_0(k)||A_d(k)|\cos(\varphi(k)) + |A_d(k)|^2. \end{aligned} \quad (1)$$

The phase difference between the zero-order beam and the diffraction beam is $\varphi(k)$. If we assume the phase

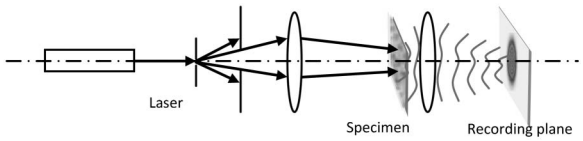

Fig. 1. Schematic diagram of the optical setup.

of the zero-order beam is zero, then $\varphi(k)$ is the phase of the diffracted beam. Mathematically, recording the diffraction patterns in the far-field plane is essentially the decomposition of the object wave into different spatial frequency components, and the reconstruction process involves the recombination of different spatial components in the real space. The existing PIE algorithm uses $\sqrt{I(k)}$ for the iterative reconstruction. However, our modified PIE algorithm considers the intensity $I(k)$ for the reconstruction. For a weakly scattering object, the zero-order beams are much stronger than the diffracted beams. This means $|A_d(k)| \ll |A_0(k)|$ and $|A_d(k)|/|A_0(k)| \approx 0$. Squaring Eq. (1) and applying these approximations, we obtain

$$I^2(k) = |A_0(k)|^2 |A_0(k) + 2A_d(k)|^2. \tag{2}$$

By doing so we get a reconstruction intensity proportional to $A_0(k) + 2A_d(k)$. Here the strength of diffracted beam $A_d(k)$, which indicates high spatial-frequency components of the object wave, is doubled relative to the zero-order beam, then the contrast of the reconstruction would be remarkably increased, and the fine details of specimen would be enhanced. To show this clearly, we draw the vectors $A_0(k) + A_d(k)$ and $A_0(k) + 2A_d(k)$ in the complex plane (Fig. 2). We assume that the polar angle of the zero-order component is zero, and the polar angle of $A_d(k)$ is assumed to be $\varphi(k)$. It is obvious that $A_0(k) + 2A_d(k)$ has a longer vector length and a larger polar angle. This means that the reconstruction with the above discussed method will result in a large phase range. Such a large phase range is more desirable since the probe diffraction pattern gets modified only slightly by the weakly diffracting specimen. This method makes the phase change very conspicuous, leading to a better contrast and visual information of the specimen.

The validity of the above analysis is verified by a numerical simulation and experiment. Figure 3(a) is the phase transmit function of a pure phase object chosen for simulation. Figure 3(b) is the intensity of the far-field diffraction patterns calculated. Since divergent illumination is used and the object is quite weakly diffracting, the zero-order beam irradiates a remarkable portion of the area in Fig. 3(b). This is in fact required to make the assumption that $|A_d(k)| \ll |A_0(k)|$. To simulate a real experimental situation, some random noise (e.g., dark current noise of CCD) is added to the diffraction pattern. Figure 3(c) is the reconstruction with common PIE method, using the square root of intensity obtained in Fig. 3(b). We can find that the structural information of the object is lost in the dominant noise. Figure 3(d) is the image reconstructed with our modified algorithm and it shows the phase structure of Fig. 3(a). We can find that it

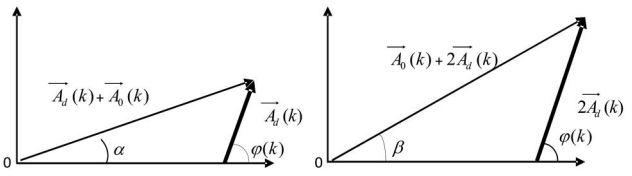

Fig. 2. Vectors $A_0(k) + A_d(k)$ and $A_0(k) + 2A_d(k)$ in the complex plane.

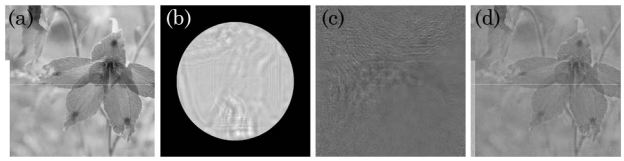

Fig. 3. Numerical simulation results. (a) The phase transmission of the object; (b) the diffraction pattern; (c) the reconstructed image with common PIE method; (d) the reconstructed image with our suggested method.

is difficult to reconstruct the weak phase object with the square root of intensity patterns because of the noise added, while the modified algorithm we have suggested faithfully reproduced the structures of the object. This result matches our above analysis well and demonstrates a higher degree of noise tolerance.

Using the same method in deducing Eq. (2), we can get $I^n(k) \approx |A_0(k)|^n |A_0(k) + nA_d(k)|^n$, $n = 2, 3, 4\ldots$. In theory, we can then do the reconstruction by using the n power of the modulus of the recorded data $(\sqrt{I(k)})^n$ to further enhance the image contrast. However, this does not mean that the contrast can be strengthened infinitely because while the diffraction beam changes from $A_d(k)$ to $2A_d(k)$, $3A_d(k)$ etc., it becomes closer to $A_0(k)$ in intensity, and then as a result, the requirement $|A_d(k)| \ll |A_0(k)|$ in Eq. (2) will not be fulfilled.

The experimental results are shown in Fig. 4. The object used is a fixed biological sample (corn stem cross-cut), and its phase distribution is quite weak. In the experiment the diffraction patterns $I(k)$ are recorded with the setup of Fig. 1. Figure 4 shows both phase image and corresponding intensity images reconstructed from $\sqrt{I(k)}$, $I(k)$, and $(\sqrt{I(k)})^3$, respectively. From Fig. 4, we can find that almost no useful structural information of the object can be identified from the reconstructed phase image with $\sqrt{I(k)}$. When making the reconstruction with the modified algorithm however, the image contrast obviously becomes better and the fine structures of the sample are remarkably enhanced. It is clear that our proposed PIE algorithm results in a better contrast and edge detection compared to the standard PIE techniques which use $\sqrt{I(k)}$ for the reconstruction.

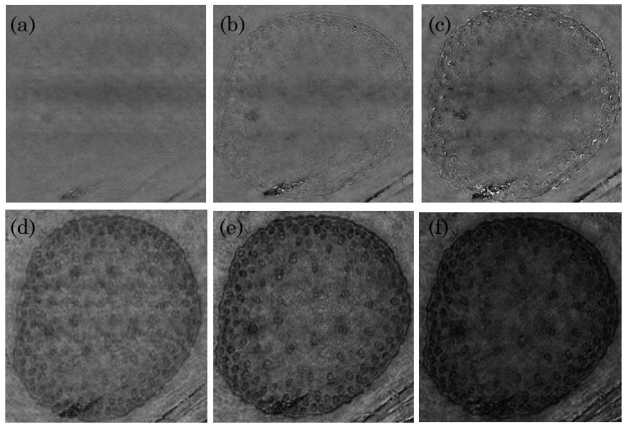

Fig. 4. Experimental results. (a)–(c) Phase and (d)–(f) corresponding intensity imagereconstructions with, $\sqrt{I(k)}$, $I(k)$ and $(\sqrt{I(k)})^3$, respectively.

Many samples used in the electron or x-ray microscopy are weakly scattering objects, and the reconstructions always suffer from the low image quality. In pursuit of better image contrast for PIE or the other CDI techniques in imaging weakly scattering objects, an optical setup for the data recording and a corresponding algorithm for the image reconstruction is proposed in this paper. The strength of the diffraction beam is doubled compared to the common algorithms being used in CDI techniques, and the image contrast is obviously enhanced. The result of this paper explains a phenomenon that has confused the researchers for many years: even though the CDI imaging theory requires using the square root of the recorded data, in practical experiments of x-ray imaging, a reconstruction with $(\sqrt{I(k)})^n$ can have better contrast for some cases [13]. Here n can be 1.2, 1.3, or other values a little greater than 1.0. This paper explains the underlying physics of such a reconstruction thereby enhancing the visual information on the specimen to a great extent.

Reference

1. J. Miao, C. Charalambous, J. Kirz, and D. Sayre, Nature **400**, 342 (1999).
2. U. Weierstall, Q. Chen, J. Spence, M. Howells, M. Isaacson, and R. Panepucci, Ultramicroscopy **90**, 171 (2002).
3. J. R. Fienup, Appl. Opt. **21**, 2758 (1982).
4. J. Spence, U. Weierstall, and M. Howells, Philos. Trans. **360**, 875 (2002).
5. H. He, S. Marchesini, M. Howells, U. Weierstall, G. Hembree, and J. C. H. Spence, Acta Crystallogr. Sect. A **59**, 143 (2003).
6. D. Shapiro, P. Thibault, T. Beetz, V. Elser, M. Howells, C. Jacobsen, J. Kirz, E. Lima, H. Miao, A. M. Neiman, and D. Sayre, Proc. Natl. Acad. Sci. USA **102**, 15343 (2005).
7. M. A. Pfeifer, G. J. Williams, I. A. Vartanyants, R. Harder, and I. K. Robinson, Nature **442**, 63 (2006).
8. H. N. Chapman, A. Barty, S. Marchesini, A. Noy, S. P. Hau Riege, C. Cui, M. R. Howells, R. Rosen, H. He, J. C. H. Spence, U. Weierstall, T. Beetz, C. Jacobsen, and D. Shapiro, J. Opt. Soc. Am. A **23**, 1179 (2006).
9. J. M. Rodenburg, Adv. Imaging Electron Phys. **150**, 87 (2008).
10. J. M Rodenburg, A. Hurst, and A. Cullis, Ultramicroscopy **107**, 227 (2007).
11. J. M. Rodenburg, A. C. Hurst, A. G. Cullis, B. R. Dobson, F. Pfeiffer, O. Bunk, C. David, K. Jefimovs, and I. Johnson, Phys. Rev. Lett. **98**, 034801 (2007).
12. M. J. Humphrey, B. Kraus, A. C. Hurst, A. M. Maiden, and J. M. Rodenburg, Nat. Comms. **3**, 730 (2011).
13. Z. Fucai and J. M. Rodenburg, Phys. Rev. B **82**, 121104 (2010).